HHS Public Access

Author manuscript

Neuroscience. Author manuscript; available in PMC 2016 September 10.

Published in final edited form as:

Neuroscience. 2015 September 10; 303: 1–15. doi:10.1016/j.neuroscience.2015.05.081.

Activation of the antigen presentation function of mononuclear phagocyte populations associated with the basilar membrane of the cochlea after acoustic overstimulation

Weiping Yang[a,b], **R. Robert Vethanayagam**[a], **Youyi Dong**[a,1], **Qunfeng Cai**[a,2], and **Bo Hua Hu**[a,*]

Weiping Yang: yangwp301@126.com; R. Robert Vethanayagam: rvr@buffalo.edu; Youyi Dong: youyidon@buffalo.edu; Qunfeng Cai: qunfengcai@gmail.com; Bo Hua Hu: bhu@buffalo.edu

[a]Center for Hearing and Deafness, State University of New York at Buffalo, Buffalo, NY 14214, USA

[b]Department of Otolaryngology and Head & Neck Surgery, Institute of Otolaryngology, Chinese PLA General Hospital, Beijing, 100853 China

Abstract

The immune response is an important component of the cochlear response to stress. As an important player in the cochlear immune system, the basilar membrane immune cells reside on the surface of the scala tympani side of the basilar membrane. At present, the immune cell properties in this region and their responses to stress are not well understood. Here, we investigated the functional role of these immune cells in the immune response to acoustic overstimulation. This study reveals that tissue macrophages are present in the entire length of the basilar membrane under steady-state conditions. Notably, these cells in the apical and the basal sections of the basilar membrane display distinct morphologies and immune protein expression patterns. Following acoustic trauma, monocytes infiltrate into the region of the basilar membrane, and the infiltrated cells transform into macrophages. While monocyte infiltration and transformation occur in both the apical and the basal sections of the basilar membrane, only the basal monocytes and macrophages display a marked increase in the expression of MHC II and CIITA, a MHC II production cofactor, suggesting the site-dependent activation of antigen-presenting function. Consistent with the increased expression of the antigen-presenting proteins, $CD4^+$ T cells, the antigen-presenting partner, infiltrate into the region of the basilar membrane where antigen-presenting proteins are upregulated. Further pathological analyses revealed that the basal section of the cochlea displays a greater level of sensory cell damage, which is spatially correlated with the region of antigen-presenting activity. Together, these results suggest that the antigen-

*Corresponding author: Bo Hua Hu, Ph.D., Center for Hearing and Deafness, State University of New York at Buffalo, Buffalo, NY 14214, USA, Phone: 001-716-829-5316; Fax: 001-716-829-2980, bhu@buffalo.edu.

[1]Department of Cell Physiology, Faculty of Medicine, Kagawa University, Kagawa, 761-0793 Japan.

[2]Department of Otolaryngology-Head and Neck Surgery, School of Medicine, Wayne State University, 252.1 Lande Bldg. 550 E. Canfield, Detroit, MI 48201 USA

presenting function of the mononuclear phagocyte population is activated in response to acoustic trauma, which could bridge the innate immune response to adaptive immunity.

Keywords

Macrophage; Cochlea; Noise; Antigen; MHC II; Immunity

Introduction

Acoustic overstimulation leads to a complex cellular response within the cochlea. This stress response is caused by initial mechanical injury and subsequent biological and molecular changes that culminate in apoptotic and necrotic cell death (Bohne et al., 2007; Han et al., 2006; Hu et al., 2000; Nicotera et al., 2001; Niu et al., 2003; Shibuya et al., 2003; Wang et al., 2002; Ylikoski et al., 2002). During this degenerative process, damaged and dead cells release various inflammatory mediators, and these inflammatory molecules activate the cochlear immune system (Fujioka et al., 2006; Nakamoto et al., 2012; Tornabene et al., 2006; Wakabayashi et al., 2010).

In the cochlea, immune cells have been identified under normal physiological conditions (Lang et al., 2006; Okano et al., 2008; Sato et al., 2008). These cells reside in the spiral ligament and the stria vascularis of the cochlea and display the macrophage phenotype (Hirose et al., 2005; Okano et al., 2008; Tornabene et al., 2006). Acoustic overstimulation causes the infiltration of circulating monocytes into the cochlea. This influx of monocytes initiates hours after cochlear injury and peaks at approximately 2–7 days after the initial damage (Fredelius, Rask-Andersen, 1990; Hirose et al., 2005; Tornabene et al., 2006; Wakabayashi et al., 2010). The infiltrated cells have been identified in various anatomic sites of the cochlea, with a marked accumulation in the spiral ligament, the scala tympani and the spiral limbus (Du et al., 2011; Hirose et al., 2005; Miyao et al., 2008; Sautter et al., 2006; Tornabene et al., 2006). In the spiral ligament, immune cells are present primarily in the region around fibrocytes (Hirose et al., 2005; Tornabene et al., 2006). The infiltrated cells are also present in the scala vestibuli, the stria vascularis, the modiolus and the spiral ganglion (Du et al., 2011; Hirose et al., 2005; Sautter et al., 2006; Tornabene et al., 2006; Wakabayashi et al., 2010), as well as beneath the basilar membrane (Tornabene et al., 2006) and on Reissner's membrane (Sautter et al., 2006). This broad distribution of the immune cells suggests the importance of the immune system in the cochlear response to acoustic injury.

Sensory cells are susceptible to various pathological insults, including acoustic overstimulation. However, the organ of Corti, which houses the sensory cells, lacks immune cell activity. Under the steady-state, the organ of Corti lacks immune cells (Du et al., 2011; Hirose et al., 2005). After acoustic injury, monocyte infiltration barely occurs to the organ of Corti (Hirose et al., 2005). By contrast, the immune cells in the surrounding cochlear partitions can respond to immune signals from the organ of Corti. The immune cells beneath the basilar membrane are adjacent to the organ of Corti. While these cells are potentially

important for immune surveillance of sensory cell damage, their response to acoustic overstimulation is not well understood.

Monocytes migrate into a target tissue in response to inflammatory signals. These infiltrated cells transform into macrophages and participate in the tissue immune reaction. Tissue macrophages are involved in three basic immune functions: phagocytosis of damaged cells, generation of inflammatory molecules, and presentation of antigens. In noise-damaged cochleae, experimental evidence for the first two functions has been reported (Fredelius, Rask-Andersen, 1990; Fujioka et al., 2006; Tornabene et al., 2006). At present, whether immune cells participate in the antigen-presenting function is not clear. Antigen presentation is an important biological process coupling innate recognition to adaptive immunity (Steinman, 1991; Unanue, 1984). Because an adaptive immune response can exert long-lasting effects on cochlear hemostasis, understanding the antigen-presenting function in the cochlear immune cells will provide important new insights into the long-term effect of acoustic stress on cochlear homeostasis and function.

In this study, we characterized the mononuclear phagocytes beneath the basilar membrane and examined their morphological and molecular responses to acoustic overstimulation. The study revealed the presence of tissue macrophages with distinct apical-basal phenotypes and protein expression profiles under steady-state conditions. After acoustic overstimulation, monocytes infiltrate into the region of the basilar membrane and transform into macrophages. We demonstrate that the monocyte transformation is time-dependent. Importantly, we found a significant increase in the expression of an antigen-presenting protein, MHC II, and its transactivator protein, CIITA, in monocytes and macrophages. Notably, the increase in the expression of these proteins occurs primarily in the basal section of the basilar membrane where greater sensory cell damage is present. Moreover, infiltration of $CD4^+$ T-cells, the antigen-presenting partner, was observed in the region where the expression of the antigen-presenting protein is upregulated. These results suggest that the activation of antigen-presenting function is an important immune cell response to acoustic trauma in the cochlea.

Experimental Procedures

The basic experiment paradigm included the following steps: a baseline hearing evaluation, acoustic overstimulation, hearing function re-evaluation, sample collection and molecular analyses. The cochlear samples were collected at 1 day, 4 days or 10 days after the noise exposure. The first two time points represent the phase of active cochlear pathogenesis and the last time point represents the phase of cochlear recovery. All noise groups had corresponding control groups, which received the same experimental treatments, except for the acoustic overstimulation. The numbers of animals or cochleae and the time points used for each set of experimental conditions will be described in the subsequent sections, as well as in Results.

1. Animals

C57BL/6J mice (male and female, The Jackson Laboratory, Bar Harbor, ME, USA) were used in this study. C57BL/6J mice were selected because this strain of mice is a commonly-

used control for genetic studies of gene functions. All mice used were 4–8 weeks old. Procedures involving the use and care of the animals were approved by the Institutional Animal Care and Use Committee of the State University of New York at Buffalo.

2. Auditory brainstem responses (ABR)

ABR measurements were conducted to assess the auditory function of the mice as previously described (Hu et al., 2012). The mice were anesthetized with an intraperitoneal injection of a mixture of ketamine (87 mg/kg) and xylazine (3 mg/kg). The body temperature was maintained at 37.5°C with a warming blanket (Homeothermic Blanket Control Unit, Harvard Apparatus, Holliston, MA, USA). Stainless-steel needle electrodes were placed subdermally over the vertex (noninverting input) and posterior to the stimulated and unstimulated ears (inverting input and ground) of the animal. The ABRs were elicited with tone bursts at 4, 8, 16, and 32 kHz (0.5 ms rise/fall Blackman ramp, 1 ms duration, alternating phase) at the rate of 21/s. The tone bursts were generated digitally (RP2.1; TDT; 100 kHz sampling rate) and fed to a programmable attenuator (PA5; TDT), an amplifier (SA1; TDT), and a closed-field loudspeaker (CF1; TDT). The electrode outputs were delivered to a pre-amplifier/base station (RA4LI and RA4PA/RA16B; TDT). The responses were filtered (100 to 3,000 Hz), amplified and averaged using TDT hardware and software. The ABR threshold was defined as the lowest intensity that reliably elicited a detectable response.

3. Noise exposure

A continuous noise (1 to 7 kHz) at 120 dB (sound pressure level, re 20 μPa) for 1 hour was used to traumatize the cochlea. This level of noise exposure was selected because it causes permanent hearing loss and sensory cell death (Cai et al., 2014), allowing us to determine the cochlear immune response to sensory cell damage. The noise signal was generated using a Real-Time signal processor (RP2.1, Tucker Davis Technologies, TDT, Alachua, FL, USA). The signal was routed through an attenuator (PA5 TDT, Alachua, FL, USA) and a power amplifier (Crown XLS 202, Harman International Company, Elkhart, IN, USA) to a loudspeaker (NSD2005-8, Eminence, Eminence, KY, USA) positioned 30 cm above the animal's head. The noise level at the position of the animal's head in the sound field was calibrated using a sound level meter (LD-PCB, model 800 B, APCB Piezotronics Div., Larson Davis, Depew, NY, USA), a preamplifier (LD-PCB, model 825, Larson Davis, Depew, NY, USA), and a condenser microphone (Larson and Davis, LDL 2559, Depew, NY, USA). The mice were individually exposed to the noise in a holding cage.

4. Cochlear tissue collection

At a defined time point before or after noise exposure (1, 4, or 10 days post-noise exposure), the animals were killed by CO_2 asphyxiation and were decapitated. The cochleae were quickly removed from the skull and then processed for cochlear dissection to collect tissues for subsequent morphological, biological and molecular analyses. A detailed description of the sample preparation and cell composition of the samples is provided in the following sections.

5. qRT-PCR

qRT-PCR was performed to determine the transcriptional expressions of CD45 and H2A-a in two separate types of tissues: the organ of Corti and the lateral wall/basilar membrane. The organ of Corti tissue contains sensory cells (inner hair cells and outer hair cells) and adjacent supporting cells (Deiters cells, pillar cells, Hensen cells, inner phalangeal cells and inner border cells). The lateral wall/basilar membrane tissue contains the mesothelial cells, the basement membrane, immune cells associated with the basilar membrane, cells of Claudius, cells of Boettcher, and all the cells in the stria vascularis and the spiral ligament.

After the animals were killed, the cochlea was quickly removed and placed in ice-cold Dulbecco's phosphate-buffered saline (PBS, GIBCO, Life Technologies, Grand Island, NY, USA). The bony shell facing the middle ear cavity was quickly removed to expose the cochlear structure. The modiolus of the cochlea was removed, but the lateral wall and the organ of Corti remained intact. Then, the tissue was placed in RNAlater solution to collect the organ of Corti tissue from the upper first cochlear turn using a technique that has been described in our previous publication (Cai et al., 2013). Then, the remaining tissue in the basilar membrane as well as the lateral wall tissues were collected using a fine needle. The isolated tissues were transferred to a small dish containing fresh RNAlater solution to wash out tissue debris from the surface of the samples. Then, the tissues were transferred to an RNase-free PCR tube and stored at −80°C until the analysis of gene expression. The tissue from one cochlea was used to generate one organ of Corti sample and one lateral wall/basilar membrane sample. There were four biological repeats for each experimental condition (noise and control).

Total RNAs were extracted from the collected tissues using the RNeasy Plus Micro Kit (Qiagen GmbH, Hilden, Germany) and were reverse transcribed using a high capacity cDNA reverse transcription kit (Applied Biosystems, Foster City, CA, USA). qRT-PCR was performed on a MyIQ two color Real-Time PCR detection system (Bio-Rad, Hercules, CA, USA). The transcriptional expression levels of CD45 and H2A-a were examined using pre-developed TaqMan gene expression primer/probe assays (Applied Biosystems). Pre-developed *Hsp90ab* and *Rpl13a* gene expression assays (Applied Biosystems) were used as endogenous controls.

6. Immunolabeling of immune proteins

Immunolabeling was performed to determine the spatial expression pattern of CD4, CD11c, CD14, CD45, CIITA, F4/80 and MHC II proteins in basilar membrane (BM) immune cells. After the animals were killed, the cochleae were collected and placed in ice-cold PBS. The round window and the oval window of the cochlea were opened with a fine needle. Through the round window, 10% buffered formalin was gently perfused into the cochlea. The cochlea was placed in the same fixative for two to four hours and then rinsed with PBS. We found no detectable difference in the immunostaining between the tissues fixed for two hours and for four hours. After fixation, the cochlea was dissected in PBS to collect the cochlear tissue under a dissection microscope. The tissues were treated with 0.5% Triton X-100 and 10 % donkey or goat serum albumin in PBS (pH 7.4) for 1 hour at room temperature. Then, the tissues were incubated overnight at 4°C with one primary antibody or two primary

antibodies (for double-labeling of two proteins, see the Results for details) at a concentration recommended by the manufacturers. The primary antibodies and their concentrations used were as follows: rat CD4 monoclonal antibody (1:20, MA1146, Thermo Inc., USA) or rabbit CD4 polyclonal antibody (1:100, NBP1-19371, Novus Inc., USA); Armenian hamster CD11c monoclonal antibody [N418] (1:100, ab33483, Abcam Inc., USA); goat CD14 polyclonal antibody (M20) (1:100, SC-6999, Santa Cruz Inc., USA); goat CD 45 polyclonal antibody (1:200, AF114, RD Inc., USA); rabbit CIITA polyclonal antibody (1:75, PA521031, Thermo Inc., USA); rat anti-F4/80 monoclonal antibody [CI:A3-1] (1:150, ab6640, Abcam Inc., USA); and rat anti-MHC Class II monoclonal antibody [NIMR-4] (1:75, ab25333, Abcam Inc., USA).

After incubation with the primary antibodies, the tissues were rinsed with PBS (3×) and incubated in the dark with one secondary antibody or two secondary antibodies for 2 hours at room temperature. The secondary antibodies included CD4 staining: Alexa Fluor® 488 anti-rat IgG, 1:100 in PBS, Invitrogen or Alexa Fluor® 488 donkey anti-rabbit IgG, 1:100 in PBS, Life technologies; CD11c staining: Alexa Fluor® 488 goat anti-armenian hamster IgG (H+L), 1:100 in PBS, Jackson Immuno Research Laboratories; CD14 and CD45 staining: Alexa Fluor® 488 donkey anti-goat IgG, 1:200 in PBS, Invitrogen; CIITA staining: Alexa Fluor® 488 donkey anti-rabbit IgG, 1:100 in PBS, Life technologies; and F4/80 and MHC Class II staining: Alexa Fluor® 488 or 594 donkey anti-rat IgG, 1:100 in PBS, Invitrogen.

After the secondary antibody incubation, the samples were rinsed in PBS and then mounted on slides with an antifade medium (Prolong® Gold antifade reagent, Invitrogen, Carlsbad, CA, USA). Certain tissues were counterstained with propidium iodide (5 μg/ml in PBS) or DAPI (1 μg/ml in PBS) in the dark for 10 min at room temperature. Both probes are DNA-intercalating fluorescent probes and were used to illustrate the nuclear morphology.

Several measures were taken to confirm the specificity of the antibodies used in this study. Western blotting was used to confirm the molecular weights of the proteins targeted by CD45 and CIITA using spleen and lymph node tissues. Both revealed protein bands that are consistent with the molecular weights of these proteins. CD4 immunoreactivity was confirmed by two different CD4 antibodies targeting different epitopes from different manufacturers. To prevent false-positive identifications, we examined the nonspecific staining of the secondary antibodies by omitting the primary antibody and found no clear fluorescence in the tissues.

7. Assessment of sensory cell damage

To determine the pattern of sensory cell damage, we quantified the number of missing outer hair cells along the organ of Corti from the apex to the base of the cochlea at 10 days after the acoustic trauma when the cochlear pathology became stable. Specifically, the animals were killed, and the cochleae were fixed in 10% buffered formalin overnight at 4°C. After cochlear dissection in PBS, the organ of Corti surface preparations were incubated with the staining solution containing Alexa Fluor 488 phalloidin (1:75; Applied Biosystems, Carlsbad, CA, USA), 0.25% Triton X-100 and 1% BSA in PBS at room temperature in the dark for 30 min. After the staining, the tissue was mounted on a slide.

8. Microscopy and image analyses

The immunolabeled tissues were first inspected using a microscope equipped with epifluorescence illumination to identify immune cells and sensory cell lesions. The entire length of the basilar membrane was photographed and the images collected were used for quantitative analyses of basilar membrane immune cells and sensory cell damage. The sites of interest were further examined with confocal microscopy (LSM510 multichannel laser scanning confocal imaging system, Zeiss, Thornwood, NY, USA) using a method that has been reported previously (Cai et al., 2014).

9. Data analyses

All experimental comparisons were statistically analyzed using SigmaStat (Version 3.5) (San Jose, CA, USA) or GraphPad Prism (Version 5) (La Jolla, CA, USA). An α-level of 0.05 was selected for significance for all statistical tests.

To quantify the expression pattern of immune molecules, we examined the positively stained cells for defined proteins. Positive cells were defined by a marked increase in immunoreactivity compared with their neighboring cells, including immune cells and mesothelial cells. To generate the cochleogram for the distribution of macrophages/monocytes along the basilar membrane, we first counted the number of CD45 positive cells for each unit distance (either 100 μm or 600 μm) of the basilar membrane for each cochlea. Then, the numbers were averaged to generate the mean values. The mean values were presented as a function of the percentage distance from the apex to the base of the cochlea. To compare the distribution pattern of positive cells along the length of the basilar membrane, we divided the basilar membrane into the apical section (0 to 42.5% from the apex) and the basal section (42.5 to 85% from the apex) using an image analysis software (ImageJ), The numbers of positively-stained cells were averaged separately for the apical region and the basal section for each cochlea. Then, the mean values were averaged to generate the group means (the apical group and the basal group) and Student's *t* test was used to compare the group means.

To quantitatively analyze the level of sensory cell damage, we quantified the number of missing outer hair cells. The sites of missing hair cells were identified by a lack of phalloidin staining in the cuticular plates. Because outer hair cells are well organized in the organ of Corti, the number of cuticular plate regions that lacked phalloidin staining could be easily identified and quantified. Each organ of Corti was thoroughly examined from the apex to the base of the cochlea. The number of missing outer hair cells was documented along the entire length of the organ of Corti, and the data were assembled into cochleograms. Student's *t* test was used to compare the number of missing outer hair cells between the apical and basal sections and between the control and noise groups.

Results

1. Tissue macrophages were present beneath the basilar membrane under steady-state conditions

The organ of Corti contains sensory cells and supporting cells, which are the major target of acoustic insults. While immune cells in the cochlea have been reported before (Hirose et al., 2005; Lang et al., 2006; Okano et al., 2008; Sato et al., 2008), the distribution of immune cells beneath the basilar membrane has not been characterized. We therefore began our study by examining the distribution pattern of the leukocytes on the surface of the scala tympani side of the basilar membrane between the lateral wall and the osseous spiral lamina (Fig. 1A).

Leukocytes were visualized using the immunolabeling of CD45, a receptor tyrosine phosphatase presenting on all hematopoietic/bone marrow derived leukocytes. The number of CD45 positive cells was counted from the apical to the basal section of the basilar membrane except for the basal extreme (85–100% from the apex), where dissection damage occasionally occurred. The average number of CD45 positive cells beneath the basilar membrane (n = 7 cochleae) was 95.4 ± 16.9. These cells were scattered throughout the entire length of the basilar membrane (Fig. 1B). No cluster or distribution gap of CD45 positive cells was found. The basal section (the distance from 42.5 to 85% from the apex) had slightly more cells than the apical section (the distance from 0 to 42.5 % from the apex) (Fig. 1C, Student's *t* test, t = −2.4, df = 12, 16 P = 0.035). This observation revealed the presence of leukocytes beneath the basilar membrane under normal physiological conditions.

2. Location-specific morphologies of macrophages beneath the basilar membrane

CD45 positive cells were polymorphic and their body morphologies were site-dependent. In the apical section (0–30% from the apex), the cells were stellate in shape with a slender body and multiple long dendritic projections (Fig. 2A). The dendritic projections were thin and the cytoplasm was scarce. The nucleus had an irregular shape, with multiple lobes connected by a band of nuclear material (Fig. 2B). Starting from the region approximately 30 % from the apex (30–70% from the apex), the length of the dendritic projections shortened and the projection number was reduced (Fig. 2C). The cells displayed more cytoplasm. Farther away from the apex (70–100% from the apex), the CD45 positive cells became amoeboid in shape (Fig. 2D). The long projections disappeared. These cells had smooth irregular nuclei with a single lobe (Fig. 2E).

In addition to the cells with irregular shapes, cells with a monocyte morphology were observed (noted by the double arrow in Fig. 2F). These cells were small and round with distinct circular nuclei that occupied most of the volume of the cells. These cells were scattered along the entire length of the basilar membrane. There were fewer than 10 cells under each examined basilar membrane, much lower than the number of large irregular CD45 positive cells. Together, these observations reveal a high degree of heterogeneity of CD45 positive cell morphologies. Importantly, the morphologies are site-specific (Fig. 2G).

3. Macrophages display diverse expression patterns for immune-related proteins

We used a macrophage marker protein, F4/80(Morris et al., 1991), to confirm that the CD45 positive cells of irregular shape are macrophages. All of the CD45 positive cells with an irregular shape displayed F4/80 immunoreactivity (Figs. 3A, 3B and 3C), indicating that these cells are macrophages. The CD45 positive cells with a small round shape had diverse levels of F4/80 immunoreactivity from undetectable, weak to strong.

We then determined the expression patterns for immune proteins in CD45 positive cells. Because CD45 positive cells in the apical section of the cochlea had morphologic characteristics of dendritic cells (Steinman, Cohn, 1973), we examined the expression of three dendritic cell marker proteins; CD11c, CD14 and MHC class II (Cao et al., 2014; Kruger et al., 2004). CD11c immunoreactivity was not detectable in the immune cells in the apical section (approximately 0 to 42.5% from the apex Fig. 3D), but was detectable in the basal section (approximately 42.5 to 85% from the apex, Fig. 3E). CD14 immunoreactivity displayed a similar distribution pattern. The positive cells were not detected in the apical section, but were detected in the basal section of the cochlea (Figs. 3F and 3G). These observations suggest that the basal macrophages have dendritic cell properties.

We found strong MHC II immunoreactivity in a small fraction of leukocytes, fewer than 10 cells/per examined basilar membrane (Fig. 3H). The MHC II positive cells were scattered across entire length of the basilar membrane. In the apical section, the positive cells displayed the typical stellate shape. In the basal section, the positive cells had the typical irregular shapes. This phenotypic heterogeneity suggests the presence of distinct subpopulations of mononuclear phagocytes.

4. Intense noise causes sensory cell damage

To provide the context for the analysis of immune cell response to acoustic trauma, we examined the impact of the acoustic overstimulation on cochlear function and sensory cell viability. The mice were exposed to a broadband noise at 120 dB SPL for 1 hour. This noise exposure caused an average of 29.3 dB of the ABR threshold shift measured at 14 days post-noise exposure, suggesting permanent cochlear damage. For the assessment of sensory cell damage, the cochleae (n = 6) were collected at 10 days after the noise exposure, when the pathology of the cochleae became stable, and were stained with Alexa Fluor 488-phalloidin. The number of missing outer hair cells was quantified. The average number of missing outer hair cells in the noise damaged cochleae was significantly higher than the control cochleae (n = 6, Student's *t* test, t = −7.375, df = 11, P = 0.001, Fig. 4A). As shown in the cochleogram (Fig. 4B), the missing cells appear more frequently in the basal section of the cochlea, and the difference in the average numbers of missing cells between the apical section and the basal section is statistically significant (Fig. 4C, Student's *t* test, t = −3.375, df = 13, P = 0.005). The finding of greater sensory cell damage in the basal section of the cochlea is consistent with previous reports using similar noise conditions in mice (Harding et al., 2005; Ou et al., 2000) and this pattern of damage is possibly related to weaker antioxidant capacity in the basal end of the cochlea (Sha et al., 2001).

5. Infiltration of monocytes and reduction in mature macrophages after acoustic overstimulation

We quantified the numbers of CD45 positive cells beneath the basilar membrane and the junction of the basilar membrane and the lateral wall at three time points after exposure to the noise (1, 4, and 10 days). Compared with the normal cochleae (n = 7 cochleae), the cochleae 19 examined at 1 day post-noise exposure (n = 6 cochleae) had no significant increase in the average number of CD45 positive cells (Fig. 5A). As described above, CD45 positive cells were present beneath the basilar membrane under steady-state conditions. These cells displayed the mature macrophage morphology; that is, a large body with an irregular shape. At 1 day post-noise exposure, the number of these CD45 positive cells was lower in the middle section of the cochlea compared with that observed in the normal cochleae. By contrast, the number of CD45 positive cells showing monocyte morphology increased. As a result, the total number of CD45 positive cells observed at 1 day post-noise exposure remained unchanged.

At 4 days post-noise exposure, all cochleae (n = 5 cochleae) displayed an increase in the number of CD45 positive cells (Fig. 5A, One way ANOVA on Rank, $H = 9.4$, $df = 3$, $P = 0.024$, Dunn's method for post hoc all pairwise multiple comparison, 4 d vs. normal, $q = 2.93$, $P < 0.05$). We did not separately quantify the numbers of the newly infiltrated monocytes and the mature macrophages at 4 days post-noise exposure because of the active transformation of monocytes into macrophages at this time, which blurred the distinction between the mature macrophages and the transforming monocytes.

The number of CD45 positive cells was reduced to the pre-noise level at 10 days post-noise exposure ($P > 0.05$, the 10-day group vs. the control group). This time frame of monocyte influx is consistent with the results reported in previous studies (Fredelius, Rask-Andersen, 1990; Tornabene et al., 2006; Wakabayashi et al., 2010).

6. Noise-induced infiltration of monocytes is more prevalent in the middle and upper basal section of the cochlea

We sought to determine the major site of infiltration and how the infiltration expanded along the basilar membrane. We examined the distribution of CD45 positive cells that had the monocyte morphology at 1 day post-noise exposure. As shown in Figure 5B, large individual variation is present. Small clusters of the CD45 positive cells are present in the middle section of the basilar membrane (approximated 40 to 70% from the apex). Large clusters of the CD45 positive cells spread over a large area of the basilar membrane with more positive cells in the basal section. Surprisingly, the basal extreme (approximately 85–100 % from the apex) lacked monocytes. This observation suggests that the major site of monocyte infiltration is in the middle and the upper basal sections of the basilar membrane. This distribution pattern of monocyte infiltration is consistent with that of sensory cell damage. We also found a large number of CD45 positive cells in the junction between the basilar membrane and the lateral wall (Figs. 5C, 5D and 5E), suggesting that the monocytes observed beneath the basilar membrane migrated from the lateral wall.

7. Transformation of monocytes into macrophages

At 1 day post-noise exposure, a large number of CD45 positive cells were round and small without dendritic projection (Fig. 6A), suggesting that they were newly infiltrated monocytes. The shape and size of these cells differed from the CD45 positive cells observed under steady-state conditions that were large and had an irregular shape. At 4 days post-noise exposure, many CD45 positive cells appeared to have the body sizes that were smaller than the large CD45 positive cells observed at steady-state conditions but were larger than the small CD45 positive cells observed at 1 day post-noise exposure. These cells had fine and short dendritic projections (Figs. 6B–G). The finding of a transforming continuum between circulating monocytes and tissue macrophages suggests that the active transformation of monocytes into macrophages takes place between 1 day and 4 days after the acoustic overstimulation.

8. Acoustic trauma induces antigen-presenting activity and antigen-presenting activity is found in the area of sensory cell damage

To determine whether the antigen-presenting function of macrophages is activated after acoustic trauma, we examined the change in expression of MHC class II, an antigen-presenting cell molecule (Cresswell, 1994; Swain, 1983). We first examined the transcriptional expression of H2-Aa, a MHC II gene, in the basilar membrane/lateral tissues of normal control cochleae (n = 3) and noise damaged cochleae at 4 day post-noise exposure (n = 4) using qRT-PCR. The expression level of H2-Aa in the noise samples was significantly increased after the acoustic injury (Fig. 7A, Student's t test, t = 3.63, df = 5, P = 0.015), indicating a transcriptional increase in gene expression after the acoustic overstimulation. Next, we examined the immunoreactivity of MHC II in the macrophages. The normal control cochleae displayed only a few MHC class II positive cells scattered in the basilar membrane (see Fig. 3H). In contrast, a significant increase in the number of MHC II positive cells was observed at 4 days post-noise exposure (Fig. 7B, Mann-Whitney Rank Sum test, Student's *t* test, t = 26.0, P = 0.029). Noticeably, the MHC-II cells were largely confined to the basal section of the cochlea (approximately 42.5 to 85% from the apex, Figs. 7C and 7D). The MHC positive cells had either the small round shape or the large irregular shape, suggesting that the increase in expression occurred in both newly infiltrated monocytes and the mature macrophages.

To provide further evidence for the activation of the MHC-mediated antigen-presenting function, we examined the expression level of CIITA, a transcriptional coactivator that controls the expression of MHC-class II (Mach et al., 1994; Mach et al., 1996; Riley et al., 1995). In the normal cochleae (n = 4 cochleae), CIITA immunoreactivity was weakly distributed in the mesothelial cells as well as in a few macrophages of the basilar membrane (Fig. 8A). At 4 days after the acoustic overstimulation, however, strong CIITA immunoreactivity was found in macrophages (Fig. 8B). These CIITA cells displayed the typical morphology of transforming monocytes. This observation suggests that the increase in CIITA expression occurs in the early phase of monocyte transformation.

9. CD4$^+$ T-cells, the antigen-presenting partner, are infiltrated into the cochlea after acoustic trauma

MHC II-related antigen presentation requires the participation of CD4$^+$ T-lymphocytes (Grusby et al., 1991). To determine whether CD4$^+$ T-cells are present in the cochlea after acoustic injury, we stained the basilar membrane tissues with an antibody against CD4, a CD4$^+$ T-cell marker protein. In the normal control basilar membranes (n = 4), CD4 positive cells were largely undetectable (Figs. 9A and 9B). In contrast, CD4 positive cells were identified in the cochleae collected at 4 days after the noise exposure (23 ± 6; n = 4, Figs. 9C and 9D). A majority of these CD4 positive cells had the T-cell morphology: small spherical or ovoid shape with a round or ovoid nucleus that occupied a large portion of the cell area. They were present primarily in the basilar membrane section from 30% to 90% from the apex, consistent with the region showing MHC II immunoreactivity. A double-staining with F4/80, a macrophage/monocyte marker, revealed that the CD4 positive cells lacked F4/80 immunoreactivity (Figs. 9E and 9F), confirming that these cells were not macrophages or monocytes. Together, these observations indicate that T-cells migrate to the basilar membrane region after acoustic injury.

10. The organ of Corti lacks immune cell infiltration

The sensory cells in the organ of Corti are the major target of acoustic trauma. However, reports on the infiltration of macrophages into the organ of Corti are inconsistent, possibly due to the difference in the magnitudes of acoustic trauma induced by different research groups. We wanted to know whether macrophages could migrate into the organ of Corti at the current level of acoustic trauma. To this end, we examined the organ of Corti for CD45 positive cells and found no CD45 positive cells in this organ in either the normal cochleae (n = 8 cochleae) or noise-damaged cochleae (1 and 4 days, n = 8 cochleae for each condition). To confirm this result, we examined the transcriptional expression level in CD45 in the tissues of the organ of Corti, which contained only sensory cells and supporting cells, by qRT-PCR. CD45 expression was not detected in the organ of Corti under the normal or the noise condition (1 and 4 days post-noise exposure; n = 4 for each condition). In contrast, CD45 expression was detected in the lateral wall/basilar membrane tissues of the cochleae in both control and noise conditions (1 and 4 days post-noise exposure; n = 4 for each condition). These observations suggest the absence of leukocytes infiltration into the organ of Corti at the noise conditions used here.

Discussion

This study was designed to characterize the leukocytes beneath the basilar membrane of the cochlea and to determine their functional contribution to cochlear immune response to acoustic overstimulation. We report three major findings. First, tissue macrophages are present beneath the basilar membrane under steady-state conditions. These cells display diverse morphological characteristics and protein expression patterns. Second, acoustic trauma induces a time-dependent monocyte infiltration, and the infiltrated cells undergo a site-dependent transformation into macrophages. Third, antigen-presenting function is activated in the mononuclear phagocytes after acoustic overstimulation, and this antigen-presenting activity is spatially correlated to the major site of sensory cell damage. Together,

this investigation suggests that the activation of antigen-presenting function is a major immune response of cochlear mononuclear phagocytes to acoustic overstimulation.

The cochlea has been traditionally considered as an immunologically privileged organ, isolated from the systemic immune system because of the presence of the blood-labyrinth barrier. However, emerging evidence has revealed the presence of strong immune activity under both steady-state and stress conditions. Immune cells have been identified in the spiral ligament and the spiral ganglion of the cochlea as well as around vascular structure in the stria vascularis under steady-state conditions (Hirose et al., 2005; Okano et al., 2008; Shi, 2010; Tornabene et al., 2006). Here, we report the presence of tissue macrophages beneath the basilar membrane. These cells are distributed from the apical to the basal end of the basilar membrane. This broad distribution pattern suggests that the immune surveillance covers the entire length of the basilar membrane.

An important finding of the current study is the phenotypic heterogeneity within the macrophages under physiological conditions. Noticeably, this phenotypic diversity is location-specific. Morphologically, the macrophages are dendritic in the apical section of the basilar membrane. By contrast, the cells are flat-bodied and have a stingray shape in the basal section of the cochlea. Biologically, the macrophages in the basal section express CD11c and CD14, which are both dendritic cell proteins. In contrast, the apical macrophages do not express these proteins. This observation suggests that the basal macrophages display dual characteristics of dendritic cells and macrophages. In addition, this study reveals that macrophages with the same morphology can display different protein expression patterns. Specifically, MHC II is expressed in a small fraction of the macrophages beneath the basilar membrane. Together, these observations suggest the presence of multiple subpopulations of basilar membrane macrophages. This heterogeneity may reflect the site-specific specialization of functional roles that are adopted by the cells in the apical and the basal sections of the cochlea. The functional implications of the apical and basal difference in macrophage properties are not clear. It has been documented in previous studies that the sensory cells in the basal section of the cochlea are more susceptible than the apical sensory cells to pathological insults, including ototoxicity, aging and acoustic injury (Pouyatos et al., 2009; Sha et al., 2001; Yang et al., 2013). The immune difference may contribute to this site-specific vulnerability.

While the infiltration of monocytes into the cochlea after acoustic injury has long been described, the functional role of infiltrated cells in cochlear pathogenesis and recovery is not clear. Macrophages have been implicated in the phagocytosis of damaged cells (Fredelius, Rask-Andersen, 1990) and generation of inflammatory molecules (Fujioka et al., 2006; Tornabene et al., 2006). Here, we provided several lines of evidence showing the activation of antigen-presenting function in macrophages. First, MHC II expression is upregulated after acoustic trauma. This result is consistent with a previous observation that immune challenge is able to provoke cochlear immune cells to express MHC II (Gloddek et al., 2002). MHC II is an essential component of the antigen-presenting machinery, serving as a vehicle to transfer antigens to the cell surface. Without this antigen presentation, T-cells are unable to interact with antigens in the tissue. Second, we observed an increase in the expression level of CIITA, a non-DNA binding transactivator that functions as a molecular switch controlling

both constitutive and inducible MHC-II expression (Chang et al., 1994; Steimle et al., 1994). Importantly, we found that the upregulation of MHC II and CIITA is site-dependent, occurring primarily in the basal section of the basilar membrane where sensory cell damage is prevalent. This observation suggests that the activation of antigen-presenting function is in response to sensory cell damage. Third, we found the infiltration of $CD4^+$ T-cells into the basilar membrane. This T-cell infiltration is consistent with a previous report that T-cell migration occurs after immunostimulation (Takahashi, Harris, 1988). Notably, the timing and the site of T-cell infiltration are consistent with the timing and the site of MHC II upregulation. Because the interaction of T-cells with antigens presented on antigen-presenting cells is the initial step of the activation of adaptive immunity, our study suggests that acoustic trauma can lead to the activation of the adaptive immune response. This speculation is supported by the finding of the local production of antibodies in the inner ear (Harris, 1984). Because acoustic trauma exerts long-term effects on cochlear homeostasis (Kujawa, Liberman, 2006), and because adaptive immunity could contribute to this long-term effect, future understanding of the molecular process of innate/adaptive transition in the cochlear immune cells will provide new insights into the cochlear responses to acoustic overstimulation.

The entry site of monocytes into the region of the basilar membrane is not completely clear. The source of monocyte entry into the cochlea is the spiral modiolar vein and its tributaries (Harris et al., 1990). The lateral wall may also serve as a major source because of the abundant vasculature in the stria vascularis and the spiral ligament of the lateral wall. In this study, we found monocyte clusters in the junction of the basilar membrane and the lateral wall. This observation suggests that the source of the monocytes in the basilar membrane is the lateral wall.

Once monocytes migrate into the cochlea, they undergo an activation process and differentiate into macrophages. The activation site of the basilar membrane monocytes has not been investigated. Our finding of a transforming continuum between circulating monocytes and tissue macrophages suggests that the transformation and activation occurs locally beneath the basilar membrane. Importantly, the functional activation of the monocytes is associated with the location of the cellular residence. Specifically, the basal macrophages display the activation of antigen-presenting function. This heterogeneity of phenotype may reflect the specialization of individual macrophage populations within their microenvironments.

Acknowledgments

This research was supported by NIDCD 1R01DC010154 to BH Hu.

Abbreviations

MHC	major histocompatibility complex
ABR	auditory brainstem response
qRT-PCR	quantitative reverse transcription-polymerase chain reaction

PBS	phosphate-buffered saline
BSA	bovine serum albumin
FPKM	Fragments per kilobase of transcript per million fragments mapped
BM	basilar membrane

References

Bohne BA, Harding GW, Lee SC. Death pathways in noise-damaged outer hair cells. Hear Res. 2007; 223:61–70. [PubMed: 17141990]

Cai Q, Wang B, Patel M, Yang SM, Hu BH. RNAlater facilitates microdissection of sensory cell-enriched samples from the mouse cochlea for transcriptional analyses. J Neurosci Methods. 2013; 219:240–251. [PubMed: 23958750]

Cai Q, Vethanayagam RR, Yang S, Bard J, Jamison J, Cartwright D, Dong Y, Hu BH. Molecular profile of cochlear immunity in the resident cells of the organ of Corti. Journal of Neuroinflammation. 2014; 11:173. [PubMed: 25311735]

Cao Q, Wang Y, Wang XM, Lu J, Lee VW, Ye Q, Nguyen H, Zheng G, Zhao Y, Alexander SI, Harris DC. Renal F4/80+CD11c+ Mononuclear Phagocytes Display Phenotypic and Functional Characteristics of Macrophages in Health and in Adriamycin Nephropathy. J Am Soc Nephrol. 2014

Chang C-H, Fontes JD, Peterlin M, Flavell RA. Class II transactivator (CIITA) is sufficient for the inducible expression of major histocompatibility complex class II genes. The Journal of experimental medicine. 1994; 180:1367–1374. [PubMed: 7931070]

Cresswell P. Assembly, transport, and function of MHC class II molecules. Annual review of immunology. 1994; 12:259–293.

Du X, Choi CH, Chen K, Cheng W, Floyd RA, Kopke RD. Reduced formation of oxidative stress biomarkers and migration of mononuclear phagocytes in the cochleae of chinchilla after antioxidant treatment in acute acoustic trauma. International journal of otolaryngology. 2011; 2011:612690. [PubMed: 21961007]

Fredelius L, Rask-Andersen H. The role of macrophages in the disposal of degeneration products within the organ of corti after acoustic overstimulation. Acta Otolaryngol. 1990; 109:76–82. [PubMed: 2309562]

Fujioka M, Kanzaki S, Okano HJ, Masuda M, Ogawa K, Okano H. Proinflammatory cytokines expression in noise-induced damaged cochlea. J Neurosci Res. 2006; 83:575–583. [PubMed: 16429448]

Gloddek B, Bodmer D, Brors D, Keithley EM, Ryan AF. Induction of MHC class II antigens on cells of the inner ear. Audiol Neurootol. 2002; 7:317–323. [PubMed: 12463193]

Grusby MJ, Johnson RS, Papaioannou VE, Glimcher LH. Depletion of Cd4+ T-Cells in Major Histocompatibility Complex Class-Ii Deficient Mice. Science. 1991; 253:1417–1420. [PubMed: 1910207]

Han W, Shi X, Nuttall AL. AIF and endoG translocation in noise exposure induced hair cell death. Hear Res. 2006; 211:85–95. [PubMed: 16309861]

Harding GW, Bohne BA, Vos JD. The effect of an age-related hearing loss gene (Ahl) on noise-induced hearing loss and cochlear damage from low-frequency noise. Hear Res. 2005; 204:90–100. [PubMed: 15925194]

Harris JP. Immunology of the inner ear: evidence of local antibody production. Ann Otol Rhinol Laryngol. 1984; 93:157–162. [PubMed: 6712089]

Harris JP, Fukuda S, Keithley EM. Spiral modiolar vein: its importance in inner ear inflammation. Acta Otolaryngol. 1990; 110:357–365. [PubMed: 2284910]

Hirose K, Discolo CM, Keasler JR, Ransohoff R. Mononuclear phagocytes migrate into the murine cochlea after acoustic trauma. J Comp Neurol. 2005; 489:180–194. [PubMed: 15983998]

Hu BH, Guo W, Wang PY, Henderson D, Jiang SC. Intense noise-induced apoptosis in hair cells of guinea pig cochleae. Acta Otolaryngol. 2000; 120:19–24. [PubMed: 10779180]

Hu BH, Cai Q, Hu Z, Patel M, Bard J, Jamison J, Coling D. Metalloproteinases and their associated genes contribute to the functional integrity and noise-induced damage in the cochlear sensory epithelium. J Neurosci. 2012; 32:14927–14941. [PubMed: 23100416]

Kruger T, Benke D, Eitner F, Lang A, Wirtz M, Hamilton-Williams EE, Engel D, Giese B, Muller-Newen G, Floege J, Kurts C. Identification and functional characterization of dendritic cells in the healthy murine kidney and in experimental glomerulonephritis. J Am Soc Nephrol. 2004; 15:613–621. [PubMed: 14978163]

Kujawa SG, Liberman MC. Acceleration of age-related hearing loss by early noise exposure: evidence of a misspent youth. J Neurosci. 2006; 26:2115–2123. [PubMed: 16481444]

Lang H, Ebihara Y, Schmiedt RA, Minamiguchi H, Zhou D, Smythe N, Liu L, Ogawa M, Schulte BA. Contribution of bone marrow hematopoietic stem cells to adult mouse inner ear: mesenchymal cells and fibrocytes. J Comp Neurol. 2006; 496:187–201. [PubMed: 16538683]

Mach B, Steimle V, Reith W. MHC class II-deficient combined immunodeficiency: a disease of gene regulation. Immunological reviews. 1994; 138:207–221. [PubMed: 8070816]

Mach B, Steimle V, Martinez-Soria E, Reith W. Regulation of MHC class II genes: lessons from a disease. Annual review of immunology. 1996; 14:301–331.

Miyao M, Firestein GS, Keithley EM. Acoustic trauma augments the cochlear immune response to antigen. Laryngoscope. 2008; 118:1801–1808. [PubMed: 18806477]

Morris L, Graham C, Gordon S. Macrophages in haemopoietic and other tissues of the developing mouse detected by the monoclonal antibody F4/80. Development. 1991; 112:517–526. [PubMed: 1794320]

Nakamoto T, Mikuriya T, Sugahara K, Hirose Y, Hashimoto T, Shimogori H, Takii R, Nakai A, Yamashita H. Geranylgeranylacetone suppresses noise-induced expression of proinflammatory cytokines in the cochlea. Auris, nasus, larynx. 2012; 39:270–274. [PubMed: 21794995]

Nicotera, T.; Henderson, D.; Hu, BH.; Zheng, XY. Noise exposure and mechanisms of hair cell death. In: Henderson, D.; Prasher, D.; Kopke, R.; Salvi, R.; Hamernik, R., editors. Noise Induced Hearing Loss: Basic Mechanisms, Prevention and Control. Noise Research Network Publications; London: 2001. p. 99-117.

Niu X, Shao R, Canlon B. Suppression of apoptosis occurs in the cochlea by sound conditioning. Neuroreport. 2003; 14:1025–1029. [PubMed: 12802196]

Okano T, Nakagawa T, Kita T, Kada S, Yoshimoto M, Nakahata T, Ito J. Bone marrow-derived cells expressing Iba1 are constitutively present as resident tissue macrophages in the mouse cochlea. J Neurosci Res. 2008; 86:1758–1767. [PubMed: 18253944]

Ou HC, Bohne BA, Harding GW. Noise damage in the C57BL/CBA mouse cochlea. Hear Res. 2000; 145:111–122. [PubMed: 10867283]

Pouyatos B, Gearhart CA, Nelson-Miller A, Fulton S, Fechter LD. Selective vulnerability of the cochlear Basal turn to acrylonitrile and noise. J Toxicol. 2009; 2009:908596. [PubMed: 20130768]

Riley JL, Westerheide SD, Price JA, Brown JA, Boss JM. Activation of class II MHC genes requires both the X□ region and the class II transactivator (CIITA). Immunity. 1995; 2:533–543. [PubMed: 7749984]

Sato E, Shick HE, Ransohoff RM, Hirose K. Repopulation of cochlear macrophages in murine hematopoietic progenitor cell chimeras: the role of CX3CR1. J Comp Neurol. 2008; 506:930–942. [PubMed: 18085589]

Sautter NB, Shick EH, Ransohoff RM, Charo IF, Hirose K. CC chemokine receptor 2 is protective against noise-induced hair cell death: studies in CX3CR1(+/GFP) mice. J Assoc Res Otolaryngol. 2006; 7:361–372. [PubMed: 17075702]

Sha SH, Taylor R, Forge A, Schacht J. Differential vulnerability of basal and apical hair cells is based on intrinsic susceptibility to free radicals. Hear Res. 2001; 155:1–8. [PubMed: 11335071]

Shi X. Resident macrophages in the cochlear blood-labyrinth barrier and their renewal via migration of bone-marrow-derived cells. Cell and tissue research. 2010; 342:21–30. [PubMed: 20838812]

Shibuya H, Kato Y, Saito M, Isobe T, Tsuboi R, Koga M, Toyota H, Mizuguchi J. Induction of apoptosis and/or necrosis following exposure to antitumour agents in a melanoma cell line,

probably through modulation of Bcl-2 family proteins. Melanoma Res. 2003; 13:457–464. [PubMed: 14512787]

Steimle V, Siegrist C-A, Mottet A, Lisowska-Grospierre B, Mach B. Regulation of MHC class II expression by interferon-gamma mediated by the transactivator gene CIITA. Science. 1994; 265:106–109. [PubMed: 8016643]

Steinman RM. The dendritic cell system and its role in immunogenicity. Annual review of immunology. 1991; 9:271–296.

Steinman RM, Cohn ZA. Identification of a novel cell type in peripheral lymphoid organs of mice I. Morphology, quantitation, tissue distribution. The Journal of experimental medicine. 1973; 137:1142–1162. [PubMed: 4573839]

Swain SL. T cell subsets and the recognition of MHC class. Immunological reviews. 1983; 74:129–142. [PubMed: 6226585]

Takahashi M, Harris JP. Analysis of immunocompetent cells following inner ear immunostimulation. Laryngoscope. 1988; 98:1133–1138. [PubMed: 2971844]

Tornabene SV, Sato K, Pham L, Billings P, Keithley EM. Immune cell recruitment following acoustic trauma. Hear Res. 2006; 222:115–124. [PubMed: 17081714]

Unanue ER. Antigen-presenting function of the macrophage. Annual review of immunology. 1984; 2:395–428.

Wakabayashi K, Fujioka M, Kanzaki S, Okano HJ, Shibata S, Yamashita D, Masuda M, Mihara M, Ohsugi Y, Ogawa K, Okano H. Blockade of interleukin-6 signaling suppressed cochlear inflammatory response and improved hearing impairment in noise-damaged mice cochlea. Neuroscience research. 2010; 66:345–352. [PubMed: 20026135]

Wang J, Dib M, Lenoir M, Vago P, Eybalin M, Hameg A, Pujol R, Puel J. Riluzole rescues cochlear sensory cells from acoustic trauma in the guinea-pig. Neuroscience. 2002; 111:635–648. [PubMed: 12031350]

Yang WP, Xu Y, Guo WW, Liu HZ, Hu BH. Modulation of Mcl-1 expression reduces age-related cochlear degeneration. Neurobiol Aging. 2013

Ylikoski J, Xing-Qun L, Virkkala J, Pirvola U. Blockade of c-Jun N-terminal kinase pathway attenuates gentamicin-induced cochlear and vestibular hair cell death. Hear Res. 2002; 166:33–43. [PubMed: 12062756]

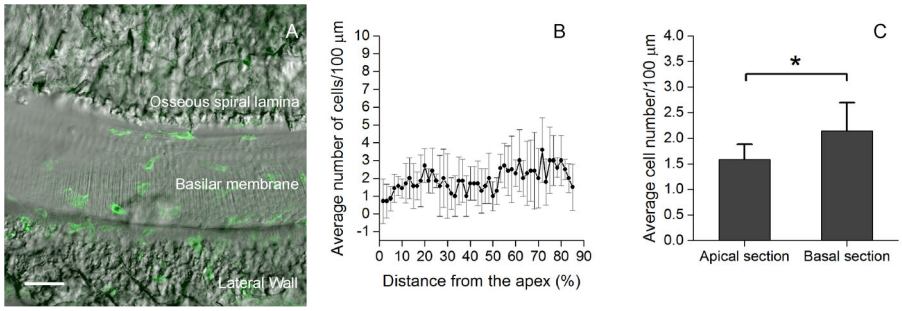

Figure 1. Distribution of leukocytes on the surface of the scala tympani side of the basilar membrane

A: The surface view of the basilar membrane of the middle cochlear turn. The CD45 positive cells (green fluorescence) are located between the osseous spiral lamina and the lateral wall. B: Distribution of CD45 positive cells along the longitudinal axis of the basilar membrane from the apex to the base of the cochlea. The data presented are the average number of the CD45 positive cells per 100-μm length of the basilar membrane (mean ± 1 SD). Notice that the CD45 positive cells are scatted over the entire length of the basilar membrane. C: Comparison of the average numbers of the CD45 positive cells/100 μm between the apical (0 to 42.5% from the apex) and the basal section (42.5 to 85% from the apex) of the basilar membrane. The number of the CD45 positive cells in the basal section is slightly, but statistically significantly, greater than that in the apical section (Student's *t* test, t = −2.4, df = 12, P = 0.035). Bar in Fig. 1A = 50 μm.

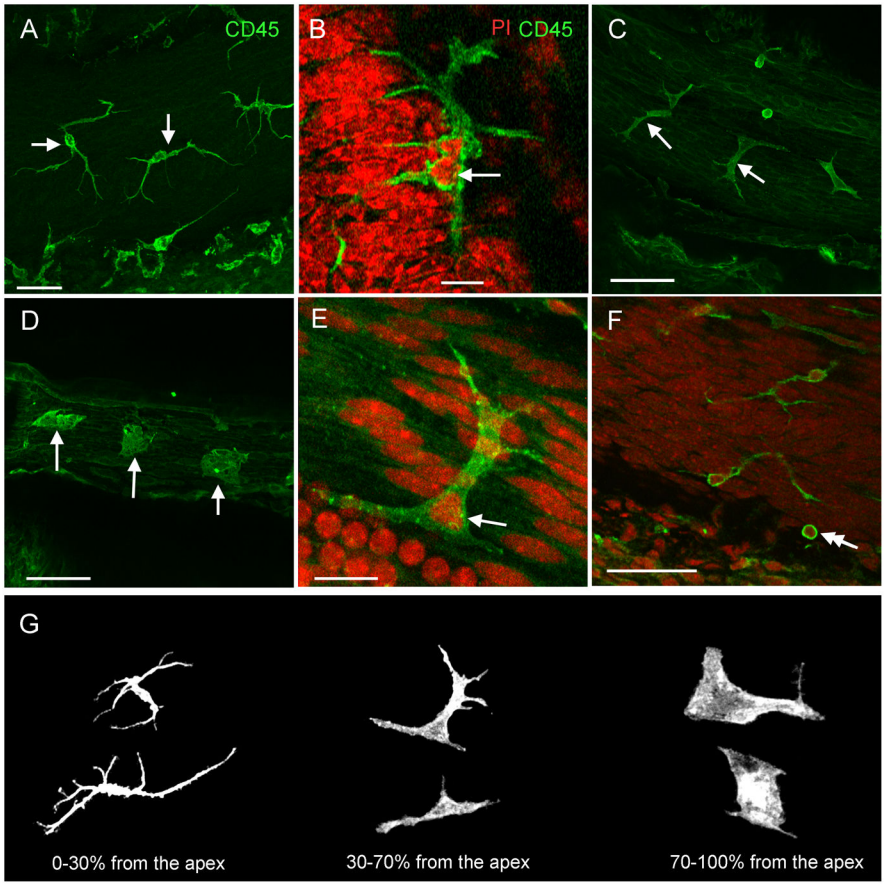

Figure 2. Distinct morphological characteristics of tissue macrophages in different sections of the basilar membrane

The tissues were stained for CD45. A: Morphology of the CD45 positive cells beneath the apical section of the basilar membrane. The CD45 positive cells display a dendritic shape with long and thin projections (arrows). B: The typical nuclear morphology of the CD45 positive cells in the apical section of the basilar membrane. The tissue was doubly stained with CD45 (green fluorescence) and propidium iodide (red fluorescence). The nucleus of the cell exhibits an irregular shape with multiple lobes (the arrow). C: Morphology of the CD45 positive cells beneath the middle section of the basilar membrane. The long projections of the cells become shortened and the volume of the cytoplasm increases (arrows). D: Morphology of the CD45 positive cells beneath the basal section of the basilar membrane. The long projections of the cells have disappeared. The cells have abundant cytoplasm (arrows). E: Typical nuclear morphology of the CD45 positive cells beneath the middle and basal sections of the basilar membrane. The arrow indicates a nucleus displaying the irregular shape with a single lobe. F: Typical morphology of the CD45 positive cells having the monocyte phenotype: a small and round cell body with a round nucleus (the double arrow). G: Summary of the morphological features of tissue macrophages along the basilar membrane from the apex to the base of the cochlea. Bars in A, C, D, and F = 50 μm, Bars in B and E = 15 μm. The images of A to F are oriented with the top being the osseous spiral lamina and the bottom being the lateral wall.

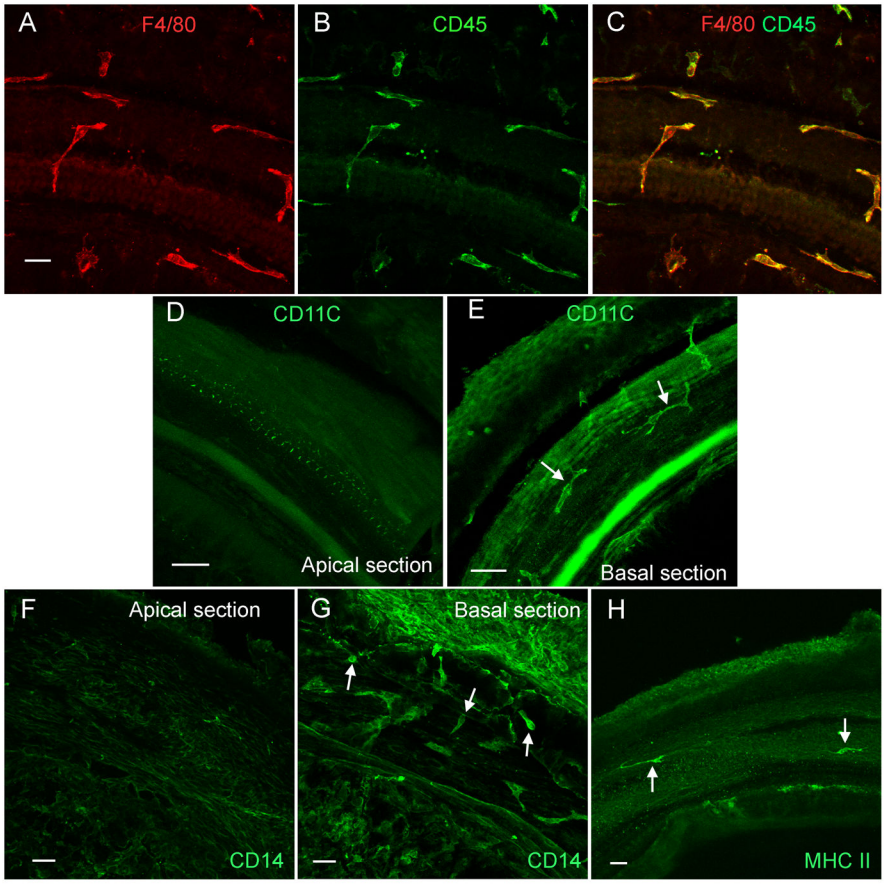

Figure 3. Expression of immune cell marker proteins

A, B, and C: Double-labeling of immune cells with F4/80 (A, red fluorescence) and CD45 (B, green fluorescence) in the middle section of a normal cochlea. All of the cells that have the irregular shape display both F4/80 and CD45 immunoreactivities (C). D and E: CD11c immunoreactivity in the macrophages beneath the basilar membrane of a normal cochlea. CD11c immunoreactivity is not detectable in the macrophages beneath the apical section of the basilar membrane (D). By contrast, the macrophages beneath the basal section display strong CD11c immunoreactivity (arrows, E). Mesothelial cells display weaker CD11c immunoreactivity. F and G: CD14 immunoreactivity in the macrophages of the basilar membrane of a normal cochlea. The CD14 immunoreactivity is not detectable in the macrophages beneath the apical section of the basilar membrane (F). Mesothelial cells display weak florescence. In contrast, the macrophages beneath the basal section of the basilar membrane display strong CD14 immunoreactivity (arrows, G). H: MHC II immunoreactivity in the macrophages of the basilar membrane. The positively stained cells (arrows) are scatted along the basilar membrane. Bars = 25 μm. All images are oriented with the top being the lateral wall and the bottom being the osseous spiral lamina.

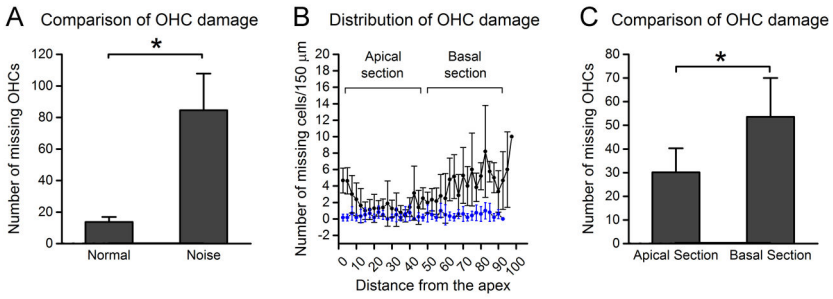

Figure 4. Distribution of outer hair cell damage after exposure to the intense noise

The cochleae were collected at 10 days after noise exposure and the missing outer hair cells were quantified. A: Comparison of the numbers of missing outer hair cells between the noise-damaged cochleae (n = 6) and the control cochleae (n = 6). The average number of missing cells in the noise-injured ears is significantly higher than in the control ears (Student's *t* test, t = −7.375, df = 11, P = 0.001), indicating that the noise level used in this study induces sensory cell damage. B: The distribution of missing outer hair cells as the function of the distance from the apex to the base of the cochlea. Notice that the missing cells appear more prominently in the basal section of the cochlea. C: Comparison of the numbers of missing cells between the apical section (0 to 42.5% from the apex) and the basal section (42.5 to 85% from the apex) of the cochlea. The average number of missing cells in the basal section is significantly higher than that observed in the apical section (Student's *t* test, t = −3.375, df = 13, P = 0.005). OHC: outer hair cells.

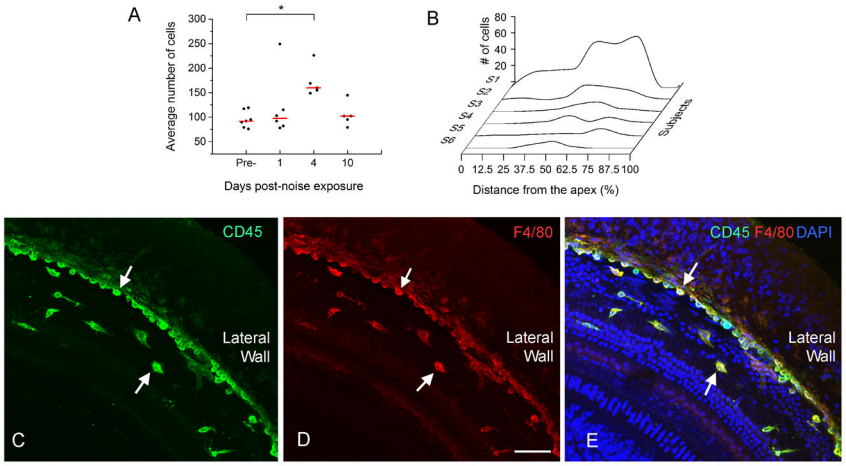

Figure 5. Infiltration of monocytes after acoustic overstimulation

A: Comparison of the numbers of CD45 positive cells between the control and three post-noise groups. The red lines represent the average numbers of the CD45 positive cells per basilar membrane of the cochlea and the dots represent the numbers of CD45 positive cells in individual samples. The mean value in the 4-day group is significantly greater than in the control group (One way ANOVA on Rank, H=9.4, df = 3, P = 0.024, Dunn's method for post hoc all pairwise multiple comparison, 4-d vs. normal, q = 2.93, P < 0.05). B: Distribution of CD45 positive cells that had the monocyte morphology along the basilar membrane of the six cochleae examined at 1 day post-noise exposure. Small clusters of the positive cells are present in the middle section of the basilar membrane (approximately 30 to 70% from the apex). Large clusters of CD45 positive cells spread toward both the apical and basal direction with more cells in the basal section. Y axis: the number of CD45 positive cells/600 μm. S1 to S6 indicate the data of individual cochleae. The data points are connected using the Akima Spline interpolation algorithm. C, D and E: A typical distribution pattern of the infiltrated monocytes in the middle section of a noise-damaged cochlea that was examined at 4 days post-noise exposure and was stained with CD45 (green fluorescence in Fig. 5C), F4/80 (red fluorescence in Fig. 5D) and DAPI (blue fluorescence in Fig. 5E). Notice that a large number of cells showing the monocyte morphology are accumulated in the juncture between the basilar membrane and the lateral wall (arrows). Bar in D = 50 μm.

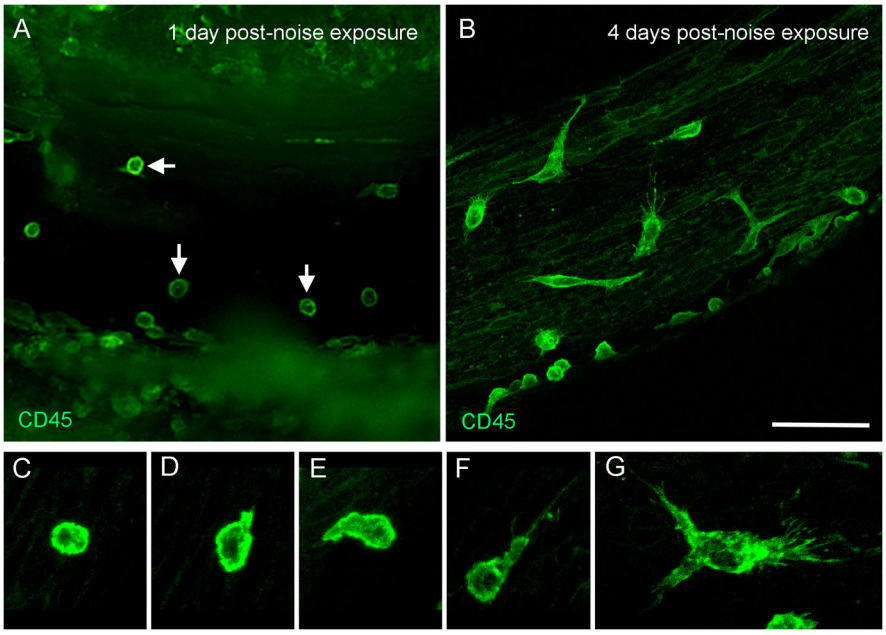

Figure 6. Transformation of monocytes to macrophages after acoustic injury

The images show the tissues that were collected from the basal half of the cochleae and were stained with CD45. A: The typical morphology of the CD45 positive cells at 1 day post-noise exposure. Notice that a large number of the cells display the monocyte morphology (arrows). The cells with irregular shapes are barely seen. B: The typical morphology of the CD45 positive cells at 4 days post-noise exposure. The cells display diverse morphologies, suggesting the active transformation from monocytes into macrophages. C to G: Transforming continuum between monocytes and macrophages. Bar in B = 50 μm. The images of A and B are oriented with the top being the osseous spiral lamina and the bottom being the lateral wall.

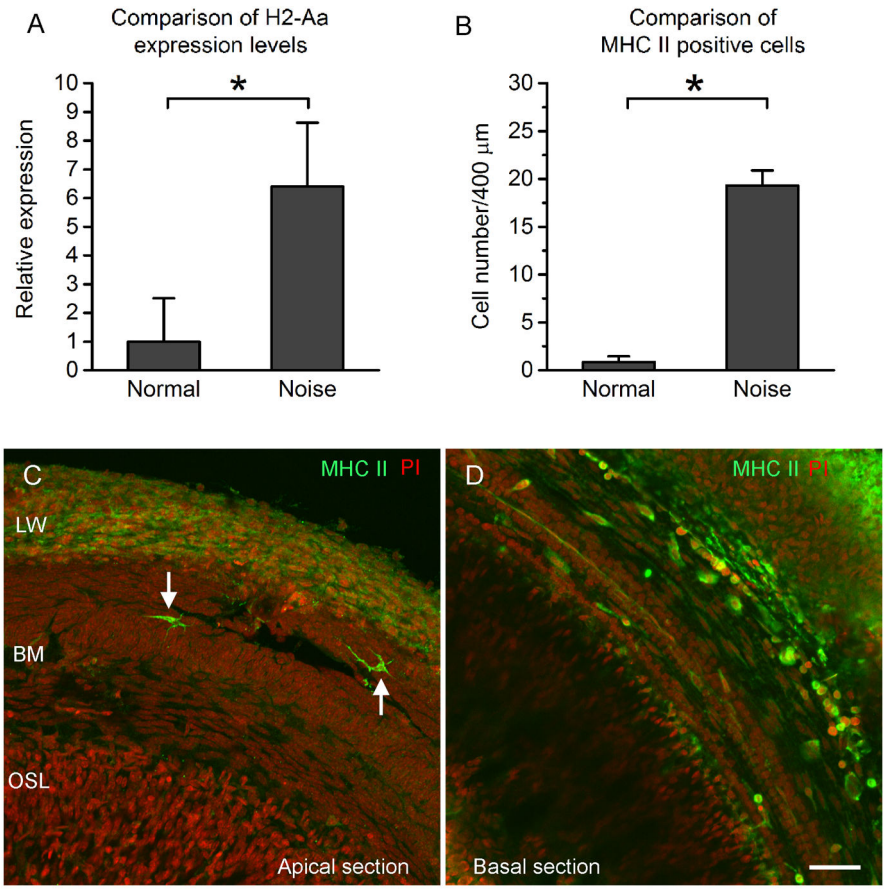

Figure 7. Expression of MHC II in monocytes and macrophages after acoustic trauma

A: Comparison of the mRNA expression levels of H2-Aa, a MHC II gene, in the basilar membrane/lateral wall tissues between the control (n = 3) and the noise samples (n = 4). The noise samples were examined at 4 day after noise exposure. The expression level of H2-Aa in the noise samples is significantly increased after the acoustic trauma (Student's *t* test, t = 3.63, df = 5, P = 0.015), indicating the transcriptional increase in gene expression after noise exposure. B: Comparison of the MHC II positive cells between the control cochleae (n = 4) and the noise-damaged cochleae examined at 4 days after noise exposure (n = 4). The average number of positive cells is significantly increased after noise exposure (a Mann-Whitney Rank Sum test, Student's *t* test, t = 26.0, P=0.029). C and D: Immunoreactivity of MHC II in a cochlea examined at 4 days post-noise exposure. The cochlea was stained with MHC II (green fluorescence) and propidium iodide (PI, red fluorescence). In the apical section (C), only a few MHC II positive cells are present (arrows). These positive cells display the typical dendritic shape. This distribution pattern of the positive cells beneath the apical section of the basilar membrane is similar to that observed in the control cochleae (see Fig 3H). In contrast, a large number of MHC II positive cells are present beneath the basal section of the basilar membrane (D), suggesting a location-specific increase in MHC II expression in the macrophages beneath the basilar membrane. Bar = 50 μm. LW = the lateral wall. BM = the basilar membrane. OSL = osseous spiral lamina.

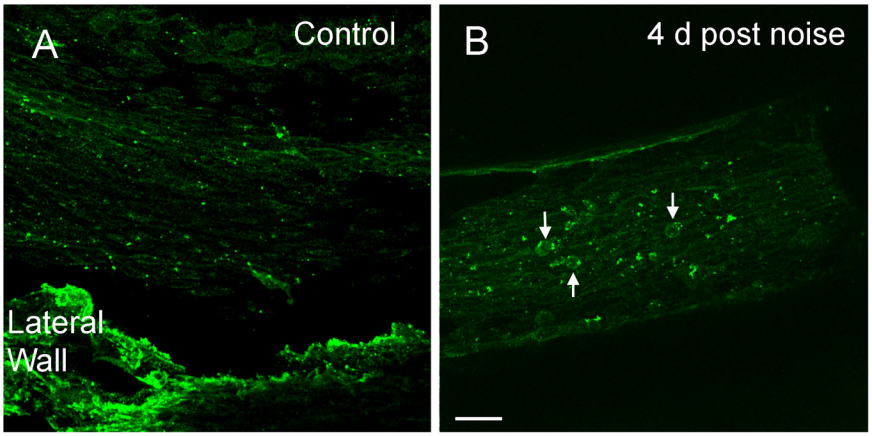

Figure 8. Expression of CIITA after acoustic trauma

A: A typical image shows the immunoreactivity of CIITA in the basilar membrane of the basal section of a control cochlea. Macrophages lack the immunostaining. Mesothelial cells on the basilar membrane display weak immunoreactivity. The tissue in the bottom of the image is the residual lateral wall tissue, which is not the focus of the current study. B: Immunoreactivity of CIITA in the basilar membrane of the basal section of a noise-damaged cochlea examined at 4 days after noise exposure. Arrows indicate the macrophages with increased CIITA immunoreactivity.

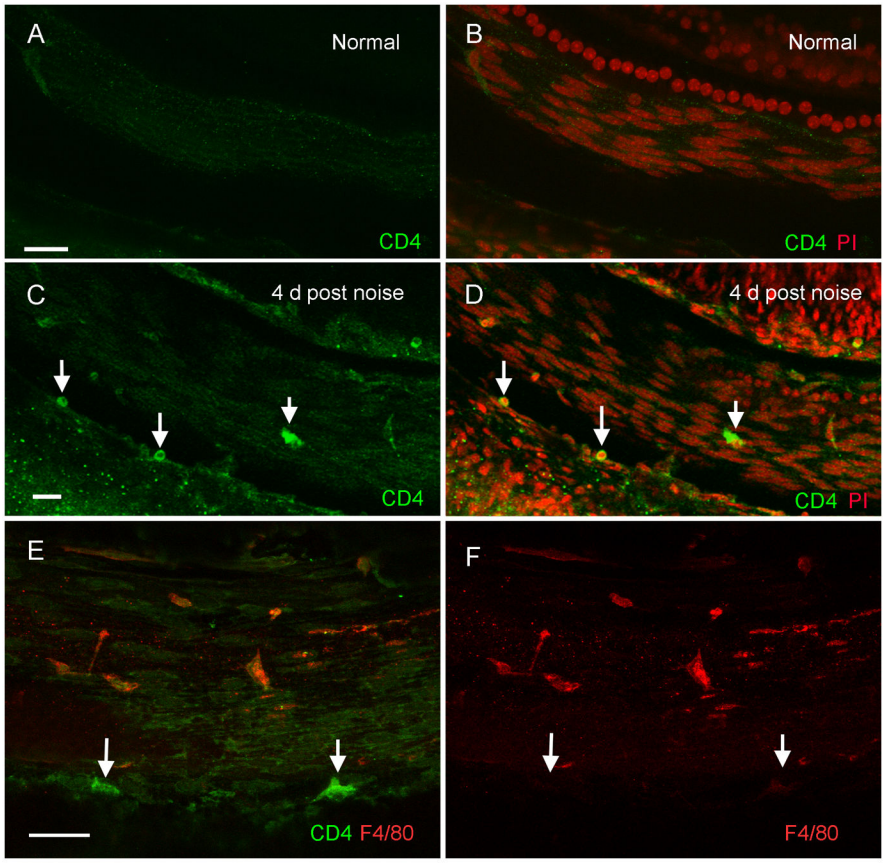

Figure 9. Immunoreactivity of CD4 in normal and noise-damaged cochleae

The images show the basilar membrane of the basal section of cochleae. A and B: CD4 immunolabeling of the basilar membrane of a control cochlea. To illustrate the tissue structure, the sample was doubly stained with CD4 (green fluorescence) and propidium iodide (PI, red fluorescence). No CD4 positive cells are present in the normal cochlea. C and D: CD4 immunolabeling in a noise-damaged cochlea at 4 days after noise exposure. Arrows indicate the CD4 positive cells. Many of these cells are small and in round shape, the typical T cell morphology. E and F: Double labeling of CD4 (green fluorescence) and F4/80 (red fluorescence) in a basilar membrane examined at 4 days after noise exposure. Arrows indicate CD4 positive cells. These cells lack F4/80 immunoreactivity. Bar = 25 μm. All images are oriented with the top being the osseous spiral lamina and the bottom being the lateral wall.